

*IDDRG International Conference, Graz, Austria, May 31 - June 2, 2010*

## Fractional behaviour at cyclic stretch-bending

*W.C. Emmens\*\*\*, A.V. Kazantzis\*\*\*, J.Th.M de Hosson\*\*\*,  
A.H. van den Boogaard\**

*\* University of Twente, Enschede, the Netherlands*

*\*\* Corus RD&T, IJmuiden, the Netherlands*

*\*\*\* University of Groningen, Groningen, the Netherlands*

*Corresponding author: [w.c.emmens@utwente.nl](mailto:w.c.emmens@utwente.nl)*

**Abstract:** The fractional behaviour at cyclic stretch-bending has been studied by performing tensile tests at long specimens that are cyclically bent at the same time, on mild steel, dual-phase steel, stainless steel, aluminium and brass. Several types of fracture are observed, these are discussed, as are the underlying mechanisms. The results agree with those obtained with  $90^\circ$  bending tests, concluding that the fracture will be orientated at  $90^\circ$  if the deformation is localized into a small transverse zone. There is a relation between the formability and a certain fracture type, also microscopic examination revealed differences, but no conclusive explanation could be given

**Keywords:** cyclic bending, fracture, formability

### 1. INTRODUCTION.

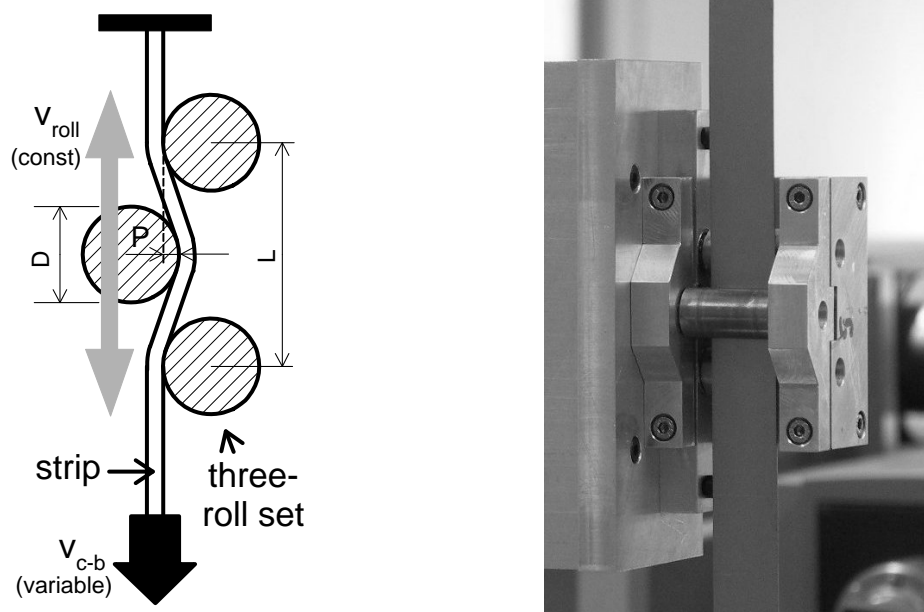
It has been known for quite some time that additional bending can improve the formability of a sheet metal. However recent developments have shown a renewed interest in this matter, and this has lead to dedicated experimental research. As the focus is on formability, fracture limits and fracture behaviour are of special interest. For example Wagoner and co-workers have performed stretch-bending tests over a single  $90^\circ$  radius, and have noticed different types of fracture [Kim *et al.*, 2009, Wagoner *et al.* 2009]. They have distinguished three types of fracture which they labelled I, II and III. Type I is a fracture as in a conventional tensile test, type III is a fracture oriented at  $90^\circ$  relative to the strip length, and type II is a mixture of both. Type I prevails at high values of  $R/t$ , and type III at low values of  $R/t$ . Similar results have been obtained by [Hudgins *et al.*, 2009]. This paper presents results obtained at cyclic stretch-bending tests with different materials. There is a general agreement with the results of Wagoner, although in the cyclic tests more types of fracture can be distinguished.

### 2. EXPERIMENTAL CONDITIONS.

The results presented here have been obtained applying the so-called Continuous-Bending-Under-Tension tests. This type of test is schematically presented in figure 1. It

has been described in detail in previous papers [Emmens and van den Boogaard, 2008, 2009] so only a brief description will be given here. Basically, a tensile test is performed on a long specimen, while at the same time a three-roll set is moving continuously up and down along the specimen with a constant speed. This type of test is in fact an incremental forming operation, where at any time the deformation is concentrated into a number of small zones: the zones where the material is actually being bent. An important characteristic of this type of test is that during bending the inner fibres are in compression. Consequently, the net pulling force is lower than in a conventional tensile test, but further depends on experimental conditions.

Only two parameters are varied: the penetration of the centre roll P (depth setting), and the cross-bar speed  $v_{cb}$  (testing speed). The depth setting simply determines the angle of bending. The testing speed determines the strain increment per passage of the roll set, and as such also the pulling force (large strain increment = large pulling force). The actual radius of bending is (much) larger than the roll radius, it is determined by an equilibrium of tension force and bending moment, and consequently governed by both the geometry (= depth setting) and the pulling force (= testing speed).



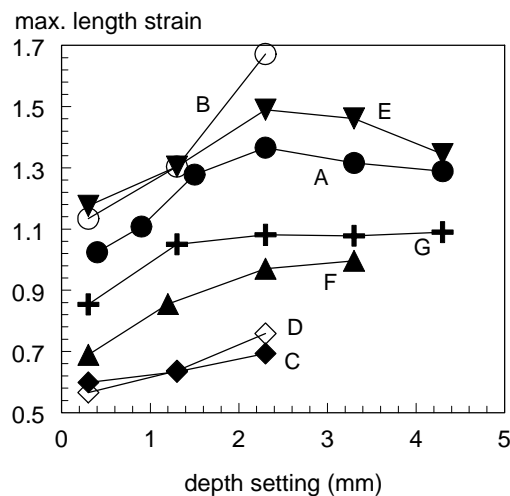
*Figure 1; Left: schematic representation of the test, right: actual roll set.  
For all tests: roll speed  $v_{roll} = 66 \text{ mm/s}$ , roll diameter  $D = 15 \text{ mm}$ , roll distance  $L = 35 \text{ mm}$ , strip width = 20 mm.*

Table I presents an overview of all tested materials, and figure 2 presents an overview of the maximum uniform elongation that has been obtained in any CBT test, for a given depth setting. Some other mild-steel variants have been tested as well, but only in a restricted number. These are not mentioned in table I or figure 2, but their results may be used below. Note that different materials show different maximum elongation, and the challenge is to find a relation with the detailed fracture behaviour. For the better under-

standing of this paper also the relation between testing speed and pulling force is important, a typical example is presented in figure 3 (compare to figure 5).

A	B	C	D	E	F	G
mild steel DC04	mild steel DC04	aluminium 5182-0	aluminium 6016-T4	stainless st. SS304	DP-steel DP600	brass 63/37 soft
0.80 mm	0.97 mm	1.15 mm	0.96 mm	0.80 mm	1.00 mm	0.69 mm

**Table I.** Overview of materials used in the tests; bottom row is thickness.



*Figure 2; Overview of maximum uniform length stain obtained in any CBT test for a certain depth setting, for all materials (see table I).*

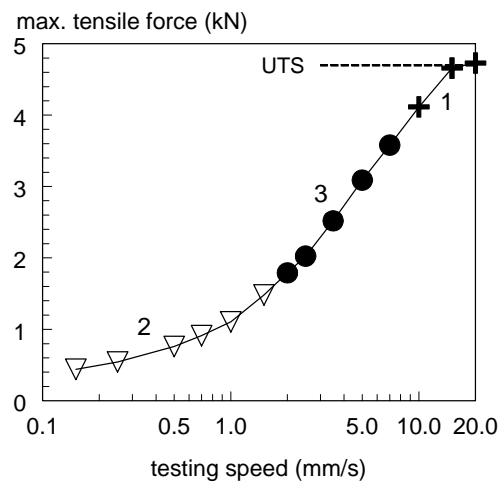


*Figure 3; Typical example of relation between testing speed and max. recorded pulling force. Symbols and numbers denote fracture type. Material: mild steel, DC04*

### 3. FRACTURE TYPES.

During the tests several types of fracture were noticed, these are briefly described here. Easily recognizable is the fracture at an oblique angle just as in a conventional tensile test, this is labelled type 1 (identical to Wagoner's type I). All other fractures are at an orientation of  $90^{\circ}$  relative to the strip length, similar to Mason's type III. Only some of all observed variants are relevant for this paper. Very characteristic is a fracture type that starts at the centre of the strip, and grows gradually outwards with successive passages of the roll set, there is no 'bang'; this is labelled type 2. Mostly occurring however is a type with a somewhat irregular fracture line, happening suddenly with a clear 'bang' and occasionally accompanied with a slight diffuse neck; this is labelled type 3. A variant of type 3 is a type that is preceded by a small local neck at  $90^{\circ}$  orientation, and has a very straight edge; this is labelled type 4. Examples of fracture types can be found in figure 4. Note that the distinction is on morphology only; the fact that the same fracture type is observed for different materials does not necessarily imply that the actual frac-

ture mechanisms are equal as well. A characteristic of this type of test is the occurrence of multiple necking and/or fracture. This is a direct consequence of the type of test and should not be interpreted as a material defect. Remember that at any time the deformation is concentrated into a small zone, because in that zone the force required for deformation is lower than in the surrounding areas. If in that zone an instability occurs a neck or fracture will develop, but as the strain is only incremented by a small value, the defect may be too small to create actual failure of the specimen. The next moment the zone of deformation has moved to an adjacent spot, that spot is now the weakest spot and the previous spot has become stronger again with the result that the defect will not grow further. As a consequence a second (or third, etc.) defect may develop at another location. Multiple necking has only been observed accompanying fracture types 2 and 4; examples are shown in figure 4.

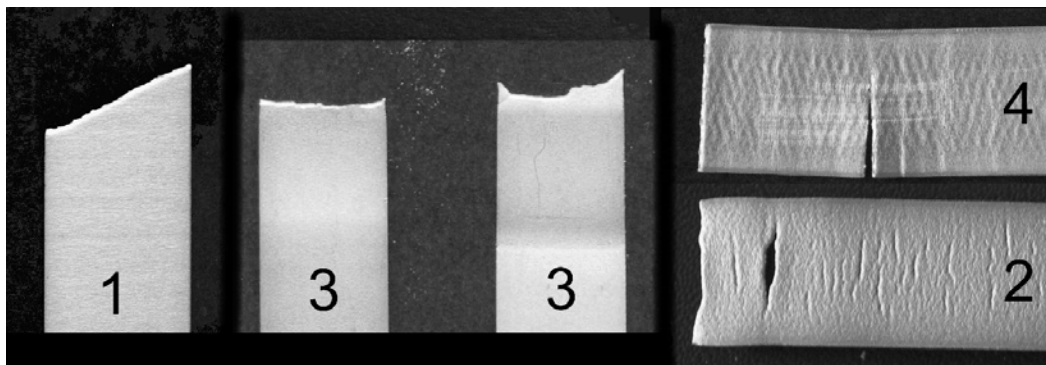


*Figure 4; Examples of fracture types (1-4). Note that the examples of type 2 and 4 are extreme cases showing multiple necking/fracture; this is not always the case.*

*Samples are not shown to the same scale.*

#### 4. RESULTS AND DISCUSSION.

For a given depth setting the formability (length strain at fracture) depends on the testing speed; a typical example of that relation is presented in figure 5. The graph shows two parts, a part where the elongation at fracture increases with increasing speed, and a part where it decreases with increasing speed; in this example the transition is at 5 mm/s. The two zones are labelled A and B. For all the experiments in this graph the recorded force-displacement curves have been converted into true-stress / true-strain curves, where the stress is the mean tensile stress over a cross-section, and the strain is the macroscopic length strain (not the cumulative bending strain). These curves are collected in figure 6. In this diagram the zones A and B form two very distinct forming limits, indicated by the two dashed lines. This also suggests that the forming limits A and B are caused by different mechanisms. These two limits will now be discussed separately.

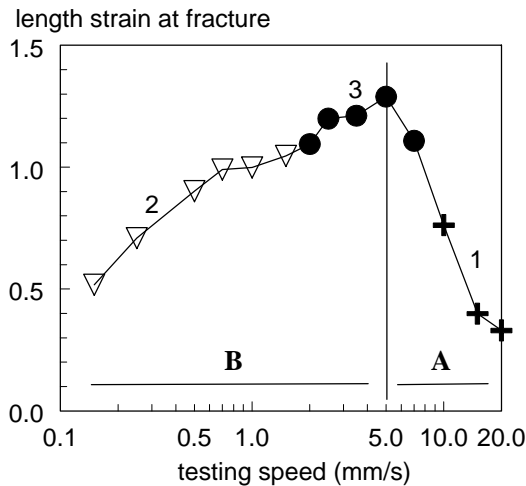


Figure 5; Length strain at fracture as a function of testing speed, a typical example. Symbols denote fracture type as indicated by the small numbers 1, 2 and 3. Material: mild steel, DC04

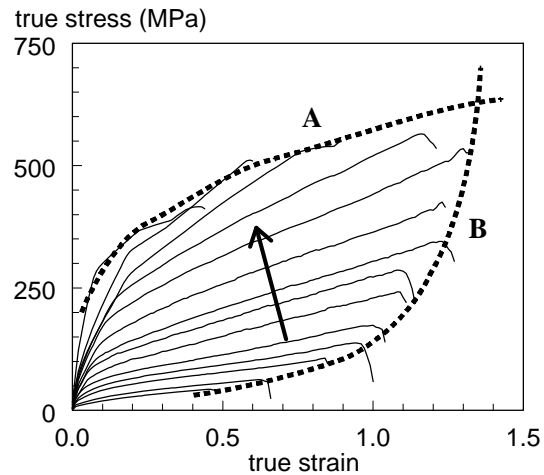


Figure 6; Collected stress-strain curves for the tests from figure 5. The kink at the end of the curves is caused by the smoothing procedure. The arrow indicates the direction of increase of speed

#### 4.1. Results - Limit A.

The following facts have been derived from the experiments concerning limit A.

A. All fractures of type 1 fall on limit A. The reverse is not true: limit A also shows fracture types 3 and 4 occasionally.

B. The stress and strain for limit A as shown in figure 5 agree with the normal hardening relation for the material. The latter has been determined by carrying out additional, conventional tensile tests on small samples taken from fractured specimens. These are not presented here in detail, but some results are shown in the preceding paper [Emmens *et al*, 2008]. This relation has been established for all materials tested so far.

C. The occurrence of fracture type 1 is related to the pulling force, it only occurs in tests where the maximum pulling forces exceeds approx. 75% of the UTS (remember that the pulling force is reduced as the inner fibres are in compression), see figures 3 and 7.

From these observations we can deduce the governing mechanism. In the tests the inner fibres are in compression, or: the neutral line in bending still lies within the strip. During the test the strip gets thinner and thinner, meaning that after some time the neutral lines shifts out of the material. At that moment there is no part in compression any more, and the test has become a conventional tensile test. As a result of the large amount of pre-straining (hardening) an instability originates immediately, causing sudden fracture. This mechanism predicts that such a failure will always occur eventually due to the constant thinning of the material, unless the specimen fractures earlier by another mechanism (limit B, discussed below). Or: fracture occurs as soon as the mean tensile stress over a cross-section is exceeding the stress that corresponds to the elongation of the material. If the pulling speed is very high, the strain increment per passage of the roll set is also very high, and so is the pulling force (see figure 3). This means that in

extreme cases the deformation is no longer concentrated into a number of small zones, but other material, outside that zones, can deform plastically as well. In that case the tensile test behaves like a conventional test, and the fracture is just as in a conventional test (type 1). Nevertheless, it is still possible that the formability is enhanced. The typical examples in figure 5 show that at very high speeds (20 mm/s) the length strain at fracture is similar to that in a conventional tensile test, but at lower speeds it is higher, sometimes considerably, while still fracture type 1 occurs.

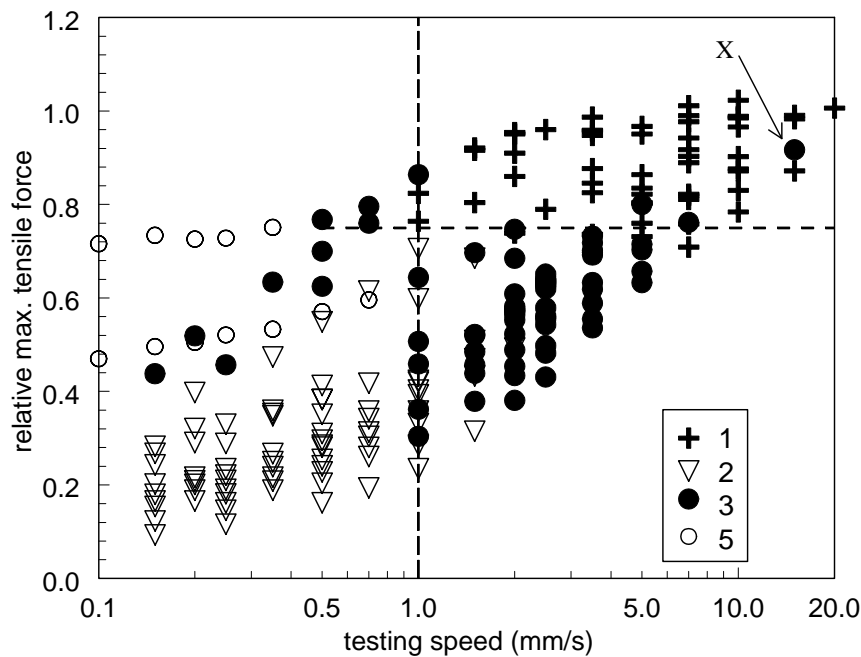


Figure 7; overview of all results obtained with mild steel and stainless steel. The relative max. pulling force is defined as the max. recorded pulling force divided by the material's UTS. Symbols denote fracture types.

#### 4.2. Results - Limit B.

Limit B is harder to analyse because it cannot be simply related to material properties. A relevant observation however is that fracture type 2 only occurs with some materials, more in detail: materials showing fracture type 2 have higher formability than materials not showing fracture type 2. Fracture type 2 was observed for mild steel and stainless steel, and a compilation of results is presented in figure 7. This graph also mentions a fracture type 5. This is a variant of type 3, only occurring with stainless steel, and related to the specific cyclic hardening behaviour of that material. That is not relevant for this paper, and will be ignored further on. The graph shows that various fracture types are prevailing in certain areas, indicated by the dashed lines. Fracture type 2 is dominant for pulling speeds of 1 mm/s and lower, except for tests with a very low depth setting P (see figure 1), where type 3 occurs. Fracture type 1 is dominant in all tests where the max. pulling force exceeds approx. 75% of the UTS. In other cases there is fracture type 3. Based on these observations we can now speculate the following mechanism. Basi-

cally the fracture starts at the centre of the strip and grows gradually outwards. However only for tests with very small strain increments (read: low testing speed) this is actually visible (type 2). When the strain increment is higher (read: high testing speeds), a starting crack cause failure within a single passage of the roll set, and this will be observed as an immediate fracture (type 3). At even higher testing speeds the pulling force becomes so high that the test becomes a conventional tensile test with corresponding fracture (type 1).

Brass showed a slightly lower formability than mild steel. Type 2 fracture did occur, but was restricted to tests done at medium to high depth settings. Also a variant of type 2 was noticed, where the crack did not start at the centre of the strip, but at the edge.

Dual phase steel DP600 showed an even lower formability. The fracture behaviour is comparable to that of mild steel, with the exception that type 2 fracture did NOT occur in any test; only type 1 and type 3 (including variants) were observed.

Both aluminium grades showed the lowest formability. Both grades also showed another fracture behaviour: type 4 fracture was observed in almost all tests including those at high speed that result in a high pulling force. The behaviour of aluminium differed from that of mild steel in more respects, and that will be discussed in the next section.

In both aluminium grades and in brass type 1 fracture occurred rarely at high speeds. This may be caused by the lack of strain-rate hardening, so that consequently a fracture is not preceded by a diffuse neck. Fracture is therefore instantaneous, and is often initiated by the passage of the roll set, forcing a 90° fracture line similar to type 3 or 4.

All materials however showed the following relations: for situations of constant depth setting the max. elongation increases with increasing speed, and for situations of constant speed the max. elongation increases with decreasing depth setting. Both point to the same: increasing speed means that the same elongation is reached with a lower amount of bending cycles, and a decreasing depth settings results in a larger bending radius, meaning less bending strain. So both relations suggest that limit B is related to the level of repetitive bending of the material: less bending results in more elongation.

#### **4.3 Mild steel vs. aluminium.**

It has been mentioned already that the level of hardening of the materials after testing has been measured by performing a second tensile tests on small samples taken from fractured or non-fractured specimens. These secondary tensile tests can be regarded as tensile tests on material with different levels of pre-deformation (cold working). From these tests the maximum engineering stress was determined, occurring either at fracture or as a proper maximum in the curve, and the engineering strain at force maximum. Figure 8 shows the relation between these two parameters for two materials. Based on general considerations we expect a relation as found for mild steel. The relation for aluminium differed from that, a number of samples apparently showed premature failure, in the figure for fracture strain below 3%. This particular effect has been observed for both aluminium grades, to a small degree also for brass, but for none of the other materials. Further analysis of the aluminium specimens revealed that premature failure mostly occurred at specimens tested at low pulling speeds, that consequently had been subjected to a large amount of bending cycles, and not at specimens that had been tested

at high pulling speeds. This hints to a suggestion that the bending and unbending operations create damage in the material that causes premature failure in the secondary tests, but is also responsible for the reduced formability as observed in the cyclic bending tests. To investigate this further, fractured specimens of DC04 and AA6016 have been subjected to microscopic examination.

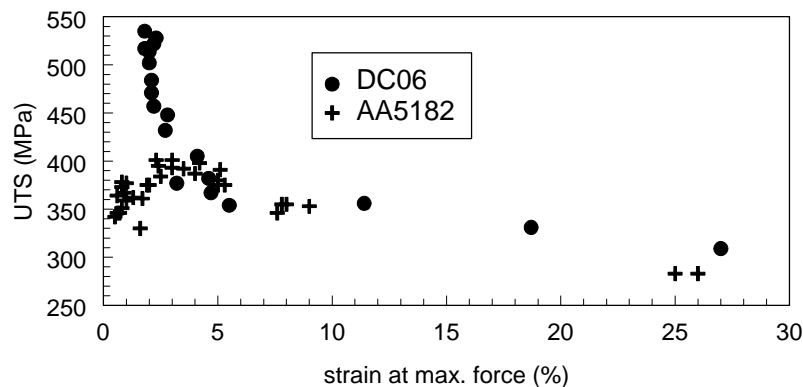


*Figure 8; relation between UTS and strain at max. force as measured in secondary tensile tests on pre-deformed specimens, for two materials.*

This investigation, performed on an XL-30S scanning electron microscope (FEGSEM), involved examination of the cross-section of the fracture surfaces, but most importantly the surfaces at the side of the specimens, just beneath their fracture cross-section. The side surfaces of aluminium specimens showed that the passage of the bending rolls flattened and spread the grains in a direction along the tensile axis (figure 9(a)). Excessive spreading, however, results in rupture of the continuity of the microstructure, resulting in large cracks perpendicular to the tensile axis. This, as well as the surface damage (cracks along the pulling direction), produced most likely by debris on the surface of the bending rolls, resulted in premature failure of these specimens. This failure was ductile, since their fracture cross-section were characterized entirely by dimples. On the other hand, the surfaces of the specimens from mild steel showed a bimodal distribution of flattened, presumably hard grains pushed inside a heavily deformed matrix that revealed a large number of wavy-like traces. The boundaries of the flattened grains appeared broken by the continuous passage of the bending rolls (figure 9(b)). The evolution of the observed microstructure can be envisaged as follows. Under the effect of bending the softer grains were deformed first; they were flattened, broken into sub-grains and forced to acquire the most easily accessible volume. The traces characterize their intensive slip occurring during their deformation. At the same time the hard grains were flattened and pushed into the surrounding microstructure comprising the initially softer grains resulting in deformation of the latter in such orientation that produced the wavy-like traces. The boundaries of the hard grains being weaker break first and are subsequently introduced into the soft heavily deformed matrix. The deformation introduced by the continuous bending reduces the thickness of the specimens but also makes the microstructure softer and capable to undergo large extensions. High bending depth, however, in-



roduces surface cracks and leads to premature failure. Examination of the fracture cross-sections showed that the specimens of mild steel failed by fatigue (figures 9(c) and (d)). All cross-sections observed showed a thin line of dimples (1<sup>st</sup> fatigue stage), followed by a striation-like intergranular failure (2<sup>nd</sup> fatigue stage) and ending in a fast transgranular cleavage (3<sup>rd</sup> fatigue stage). As a result, the fracture cross-sections, especially where cleavage was observed, were almost parallel to the tensile axis (figure 9(d)).

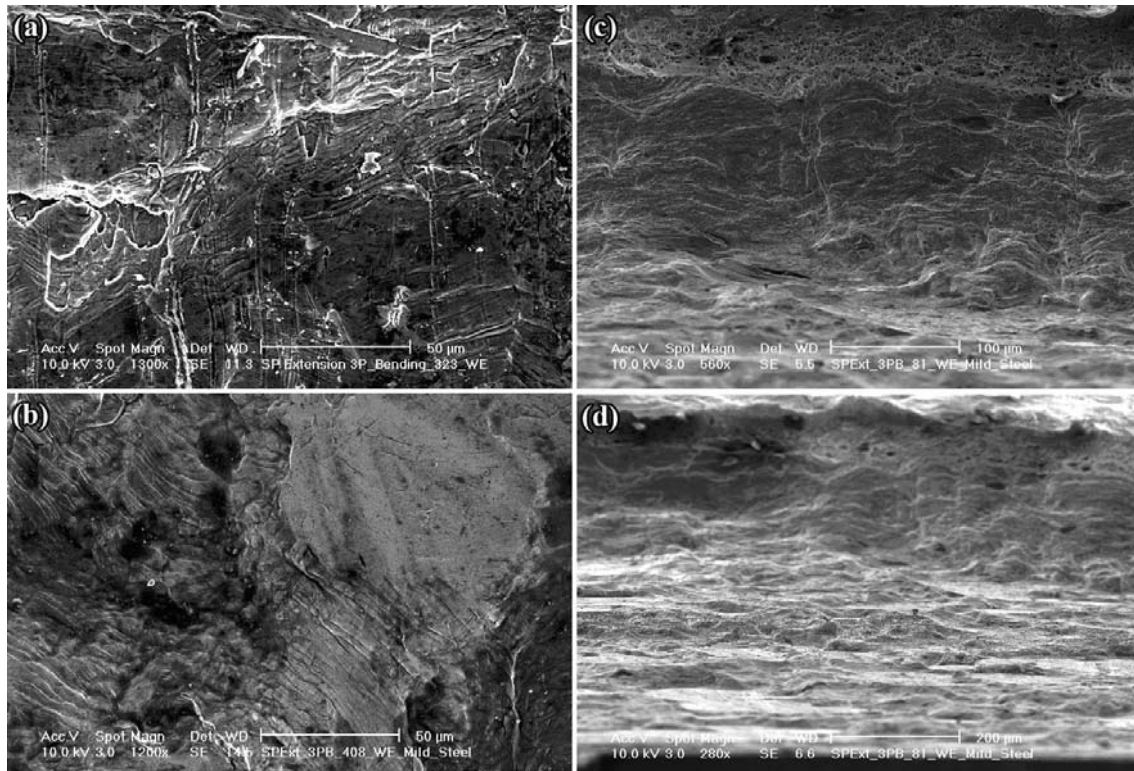


*Figure 9; (a) The side surface of an aluminium specimen showing spread grains and cracks (tensile axis from top to bottom). (b) The side surface of a specimen from mild steel showing a flattened (hard) grain within a soft microstructure with wavy like traces. (c) The fracture cross-section from a specimen of mild steel showing dimples (top) vertical striations (middle) and (d) the transgranular cleavage region.*

## 5. CONCLUDING DISCUSSION.

Several authors that have carried out 90<sup>0</sup> stretch bending tests (see introduction) have tried to explain the different fracture types in terms of micro-mechanical behaviour. However based on the results presented here another hypothesis is presented:

- *if the deformation is localized into a small transverse zone (by whatever means), the fracture will take place in that zone as wells and consequently will be oriented at 90<sup>0</sup> relative to the tensile axis.*

This simply implies that a  $90^\circ$  oriented fracture is not mysterious at all. The hypothesis is not contradicted by results obtained with  $90^\circ$  stretch bending tests. The observation of the occurrence of type 1 fracture here, and the relation with the pulling force (figure 7) substantiates this hypothesis. An even better illustration is the particular fracture marked "X" in figure 7. Based on the conditions one expects type 1 fracture. However it was noticed that at the very moment the instability would grow into a fracture, a roll was passing, again concentrating the deformation into a narrow zone. This forced the crack to lie into that zone as well, resulting in type 3 fracture.

The limit type A is reasonably well understood. The limit type B however remains obscure. One can expect that if a material is sensitive to low-cycle fatigue, it will show poor performance in this type of tests with many bending cycles. The reverse however is not true. If a material does show poor performance, it may be caused by other, possibly unknown mechanisms as well. This cannot be deduced from the fracture type. Both DP600 and mild steel show type 3 fracture, but this does not imply that the underlying mechanisms creating failure are the same. Further, microscopic examination suggested that mild steel is failing by fatigue, but did not made clear why aluminium, that is known to be more sensitive to fatigue, had a much poorer performance. There is however one very relevant observation: all materials that show type 2 fracture also show better performance (higher formability) than all materials NOT showing type 2 fracture, and brass seems a transition between these two groups of materials. A statistical relation is not necessarily also a causal relation, but it does point into a certain direction. Nevertheless, much more research is needed to get a final answer.

#### AKNOWLEDGEMENT

Part of this research was carried out under the project number K41.1.09349 in the framework of the Research Program of the Materials innovation institute (M2i) ([www.m2i.nl](http://www.m2i.nl)).

#### REFERENCES

- [**Emmens and van den Boogaard, 2008**] W.C Emmens, A.H. van den Boogaard; Extended tensile testing with simultaneous bending; *Proc. IDDRG 2008 Int. Conf., Olofström, Sweden, June 16-18 2008*, pp 219-229, ISBN 978-91-633-2948-7
- [**Emmens and van den Boogaard., 2009**] W.C Emmens, A.H. van den Boogaard; Incremental forming by continuous bending under tension - An experimental investigation; *J. Mat. Proc. Technology*, 209 (2009) pp. 5456-5463
- [**Hudgins et al., 2009**] A.W. Hudgins, D.K. Matlock, J.G. Speer; Shear Failures in Bending of Advanced High Strength Steels; *Proc. IRRDG 2009 Int. Conf, June 1-3, 2009, Golden CO, USA*, pp 53-64
- [**Kim et al., 2009**] J.H. Kim, Ji.H. Sung, R.H. Wagoner; Thermo-Mechanical Modelling of Draw-Bend Formability Tests; *Proc. IRRDG 2009 Int. Conf, June 1-3, 2009, Golden CO, USA*, pp 503-512.; ISDN 978-0-615-29641-8
- [**Wagoner et al., 2009**] R.H. Wagoner, J.H. Kim, J.H. Sung; Formability of Advanced High Strength Steels; *Proceedings Esaform 2009, Enschede, Netherlands, April 27-29, 2009*, paper 12